Discontinuous laminate composites manufactured with fiber waste

Design approaches and failure analysis

Shiino, Marcos Yutaka; Albernaz, Gabriel Guerra; dos Santos, Yasmim Bustamante; Monticeli, Francisco Maciel

DOI
10.1002/pc.29828

Publication date
2025

Document Version
Final published version

Published in
Polymer Composites

Received: 17 December 2024 | Revised: 6 March 2025 | Accepted: 8 March 2025

DOI: 10.1002/pc.29828

RESEARCH ARTICLE

spe INSPIRING PLASTICS PROFESSIONALS Polymer COMPOSITES WILEY

Discontinuous laminate composites manufactured with fiber waste: Design approaches and failure analysis

Marcos Yutaka Shiino[1] | **Gabriel Guerra Albernaz**[2] | **Yasmim Bustamante dos Santos**[2] | **Francisco Maciel Monticeli**[3]

[1]Departamento de Engenharia Ambiental, Instituto de Ciência e Tecnologia, Universidade Estadual Paulista (Unesp), São José dos Campos, Brazil

[2]Faculdade de Engenharia, Guaratinguetá, Departamento de Materiais e Tecnologia, Fatigue and Aeronautic Materials Research Group, Universidade Estadual Paulista (Unesp), São José dos Campos, Brazil

[3]Department of Aerospace Structures and Materials, Faculty of Aerospace Engineering, Delf University of Technology, Delf, The Netherlands

Correspondence
Marcos Yutaka Shiino, Departamento de Engenharia Ambiental, Instituto de Ciência e Tecnologia, Universidade Estadual Paulista (Unesp), São José dos Campos, Brazil.
Email: marcos.shiino@ict.unesp.br

Funding information
Fundação de Amparo à Pesquisa do Estado de São Paulo, Grant/Award Numbers: 2017/16160-8, 2023/08798-3

Abstract

Laminate composites are increasingly being used in the transport sector due to their lightweight structures, resulting in fuel savings. However, waste is generated in the form of post-industrial or post-consumer goods that end up in landfill or incineration. One way to minimize the impact of these disposals is through recycling or reuse, but introducing reused fibers with reduced length has been a challenge to keep the mechanical properties. In this context, this research aims to evaluate the influence of the fabric (satin weave) length on the tensile properties of discontinuous laminate and investigate the failure process of such composites manufactured with carbon fabric waste generated at the cutting process. For this purpose, two types of laminates were manufactured, each comprised of five plies (i) three continuous plies and two discontinuous plies; and (ii) one continuous ply and four discontinuous plies with varied fiber length. The laminates were tested by tensile loading, and the strain field was monitored by a non-contact technique called digital image correlation (DIC), which allowed the investigation of the local strain variation due to the interrupted section. It was possible to observe a sharp stress range in which the joint failure was evidenced by strain field variation over the joint. For both laminates, it was possible to depict the events that constrain the tensile strength of the discontinuous laminates, which is severe in laminates with surface discontinuity, and it shows to be advantageous to employ a continuous ply on both surfaces, improving loading transfer between plies.

Highlights

- Environmental problem related to carbon fiber waste from the cutting process.
- Take advantage of using small pieces of carbon fiber fabric in laminate architecture.
- Investigation of the influence of fabric disposition and fabric length on in-plane mechanical properties.
- Analysis of failure events using strain field measurements via DIC.

KEYWORDS

critical fiber length, short fiber composite, thermoplastic matrix

1 | INTRODUCTION

Currently, the transport industry is using lightweight materials as a way to improve performance, resulting in lower fuel consumption.[1] Polymers and polymer composites meet this requirement, and the latter also increase the mechanical properties, expanding their application to other fields such as energy and construction.[2,3]

The concern about the use of fossil fuels in the transportation sector increases the demand for these lightweight materials, but their origin can be mostly from finite resources such as petroleum, raising the problem of waste generation and depletion of finite resources. For example, carbon fiber reinforced polymer has carbon fiber as reinforcement which is a petroleum-based material (polyacrylonitrile-PAN as a precursor) that has been widely used in aircraft.[4,5] This fact adds a precaution when using these materials in relation to their final destination, causing some impacts in the form of either waste accumulation or greenhouse gases (GHG) emissions through landfilling or incineration, respectively.[6] For the production of carbon fiber, this is more critical as its production is energy intensive, causing impacts due to the use of electricity.[2]

The carbon fiber waste generation from the post-industrial phase is produced during the trimming operation or poor quality standards, which encompass around 30%–40% of waste stream.[2,7,8] Among the disposal options, carbon fiber recycling has more advantages, considering that all embodied energy is not lost, while other options will lose it. For example, incineration of composite would provide around 30 MJ/kg,[3] meanwhile the production of carbon fiber requires 183–286 MJ/kg,[2] providing a negative energy balance. However, recycling scrapped carbon fiber has the disadvantage of having a short length that will decrease the mechanical properties, and the application will be restricted to secondary use.[9,10]

This drawback has been investigated along the years[11] and key parameters were identified that determine the mechanical properties of short fiber composites (SFC): fiber orientation and fiber length.[12] Considering the case that the fiber is aligned to the loading direction, the strength of the composite increases if sufficient loading is transferred from the matrix to the fiber; then, for scrapped fibers with limited length (below the critical length) they will pull out from the matrix.[12,13] The called critical length (l_c) of short fiber composite is determined using Equation (1), where σ_f is the tensile strength of the fiber, d is the fiber diameter, and τ is the shear strength that acts at the interface between fiber and matrix.[11,13]

$$l_c = \frac{\sigma_f d}{2\tau}. \quad (1)$$

The main discussion in Equation (1) is the interface condition in which for the ideal one, the critical length is provided as an ideal length (minimum). However, this fiber length is higher for most combinations of fiber matrix types, suggesting that the value of shear strength is governed by interface conditions.[12,14] In addition, the shear force developed at the fiber/matrix region is considered constant along the fiber.[14,15]

In the light of the studies carried out, the main challenge is to find a balance between fiber recycling and the properties required for the project, which makes the structural design even more complex. For that purpose, this research covers the design approaches for reusing dry carbon fiber fabric from post-industrial waste with a focus on limiting tensile strength due to the sequence of stacked plies and the discontinued ply region. The analysis was based on the stress state at the surface of the flat specimens by monitoring the field strain using a non-contacting method.

2 | EXPERIMENTAL PROCEDURES

2.1 | Materials and process

Waste fabric of carbon fiber (5HS—harness satin) in the form of 0°/90° angles (areal weight of 375 g/m^2) was displaced in the mold with the discontinuities superposed by a continuous layer (overlapped discontinuity).

The layup comprised five layers in the following staking sequence: $[0/90]_5$ with 52% fiber volume fraction. Two types of design were proposed: (i) a laminate comprised of all layers with a discontinuity; and (ii) a laminate with three continuous fabrics and two discontinuous fabrics, as shown in Figures 1 and 2, respectively. The codes for both types of laminates are described in Figures 1 and 2.

Laminate type XDY (Figure 1) has a discontinuity on the surface, which means that the load transmission is interrupted by the scrapped fabric. This type of design limits the in plane tensile strength due to the raise of out-of-plane loads,[14] on the other hand it takes advantage of using more pieces of scrap fabric with a high discontinuity density per laminate of 1.4 (number of discontinuity/total number of plies). This is strategy only employs scrapped fabrics which avoids disposing the waste material in landfills or eliminate through incineration.

Laminate type XCW (Figure 1) has three continuous plies alternated by discontinuous plies as shown in Figure 2. The continuous ply shields the interrupted ply, which maximizes the in-plane tensile strength but needs to use a continuous virgin fabric or a recovered fabric that maintains the original length. This type of design avoids the problems of out-of-plane loads at the surface, thereby avoiding early failure at the surface. On the other hand, it

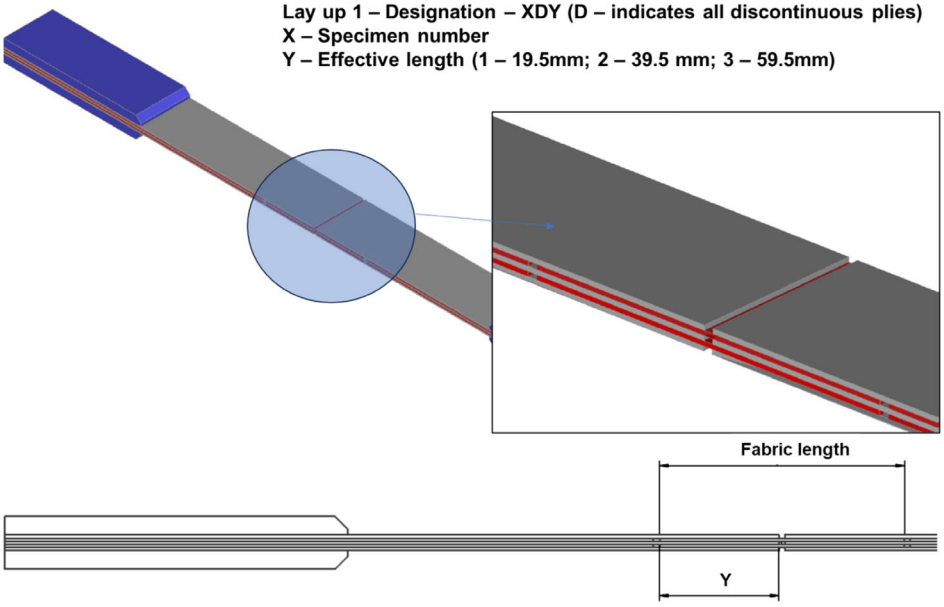

FIGURE 1 Layup with all discontinuous fabrics.

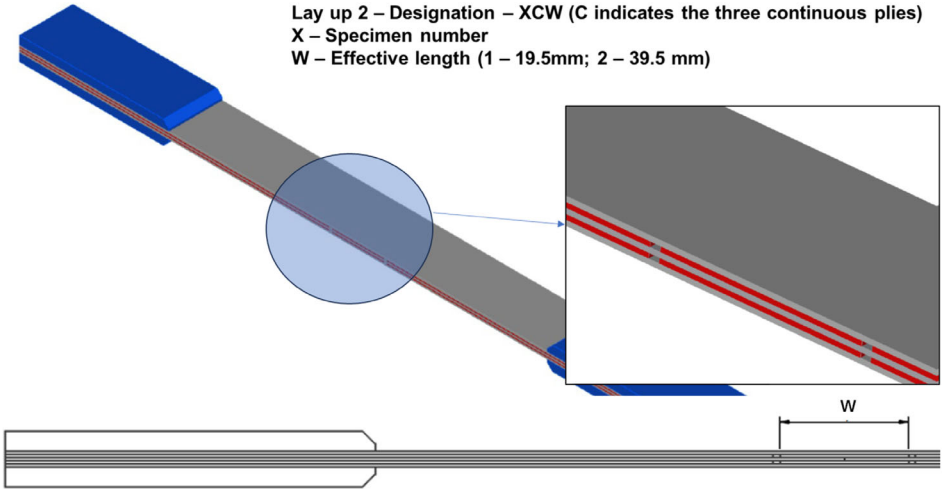

FIGURE 2 Alternated configuration.

decreases the density of discontinuity per laminate to 0.8 (number of discontinuity/total number of plies).

A saturated polyethylene terephthalate film (PET) with a thickness of 125 μm was employed as a matrix and placed in between the carbon fiber fabric. The assembled preform was then consolidated by a compression molding with a final temperature reaching 270°C and a final pressure of 130 bar (13 MPa). The mold was cooled in an environmental atmosphere that generated a cooling rate of 0.65°C/min, which provided a semi-crystalline structure.

2.2 | Tensile test setup

The final panel was sectioned in rectangle shape using a diamond saw blade cooled by water, and the final dimension of specimens was (240 × 20 × 2) mm, according to ASTM D3039-14 recommendations.[16] The specimens were sprayed with white and black color to obtain a spackled surface to monitor the strain via digital image correlation (DIC). Five specimens were prepared in each condition to be tested in tensile quasi-static load with a displacement rate of 1 mm/min conducted in a servo-mechanical test machine with a loading cell of 50 kN.

For the strain analysis, the images were achieved with an acquisition rate of one image every 5 s by employing camera CANON model EOS T3i with a 100 mm lens. The image acquisition was synchronized with the tensile test machine.

2.3 | Image analysis

The images were processed with software GOM Correlate (ZEISS Quality Suite) where it was possible to select the

maximum strain at the location of the discontinuity and at the gage section as shown in Figure 3. Every red color region was scanned to pick up the maximum strain. A representative specimen of each laminate type was selected to conduct the analysis of concentration stress around the discontinuity.

3 | RESULTS

Table 1 summarizes the results for all tests. The reference (*R*) shows the result of continuous pristine composite, which presented 523.91 ± 4.81 MPa. The laminate type XD1 indicates a residual tensile strength of 17.87% compared to the reference specimen, indicating a poor stress transfer between plies given the poor adhesion condition. The results showed that with the presence of discontinuities in all layers and with a close spacing (i.e. 19.5 mm), the stress becomes matrix domain, giving results close to the matrix fracture stress of 60–80 MPa. The increase in the distance between the discontinuities is due to a better distribution of the reinforcement material, giving an increase of 32% and 61% for 39.5 and 59.5 mm lengths compared to 19.5 mm. However, it still provides reduced

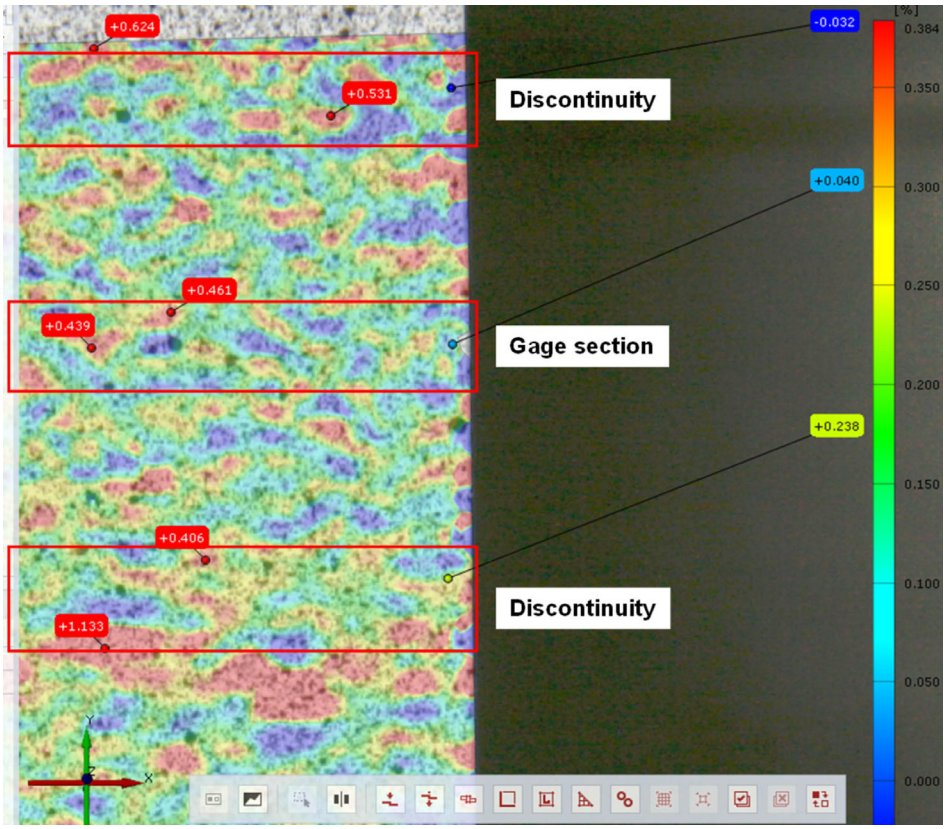

FIGURE 3 Strain field in the specimen with sub-surface discontinuity.

TABLE 1 Results of five types of discontinuous composites.

Specimen number (X)	*R* Reference	XD1 (MPa) 19.5 mm	XD2 (MPa) 39.5 mm	XD3 (MPa) 59.5 mm	XC1 (MPa) 19.5 mm	XC2 (MPa) 39.5 mm
1	524.12	99.74	116.73	151.47	304.68	379.49
2	519.05	92.42	120.59	138.23	294.68	358.35
3	528.67	95.67	128.37	146.33	365.07	368.38
4	–	86.87	131.39	151.62	414.69	364.20
5	–	–	–	169.24	357.89	430.66
Average	523.94	93.67	124.27	151.38	347.40	380.22
Std	4.81	5.43	6.78	11.37	48.87	29.24
CV	0.92%	5.80%	5.46%	7.51%	14.07%	7.69%
Residual strength	–	17.87%	23.72%	28.89%	66.30%	71.57%

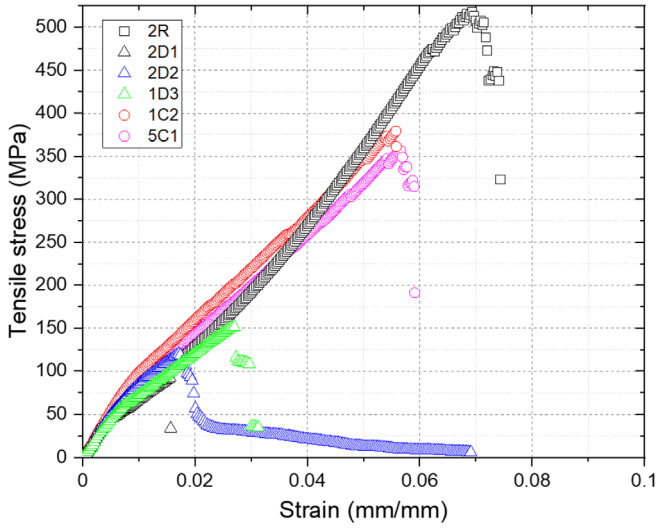

FIGURE 4 Stress–strain curves for all types of laminates.

residual strength, reaching a maximum of 23.72 and 28.89 compared with the reference.

For laminates XCW, the continuous plies at the surfaces and middle plane allowed the tensile strength to increase by providing the residual strength of 66.30% and 71.57% in relation to the reference specimen. The smaller difference between both and the greater proximity to the results of the pristine laminates indicates a dominance of the continuous layers. In addition, the smaller delta between the different discontinuity lengths indicates a lower dependence compared to the laminates with discontinuity in all layers.

Figure 4 shows the differences of the laminate types in a stress–strain curve. When dealing with composite materials, there is a characteristic scatter attributed to the tensile strength of the fiber[13] in discontinuous laminate, there could be a scatter associated with the fabric scraps

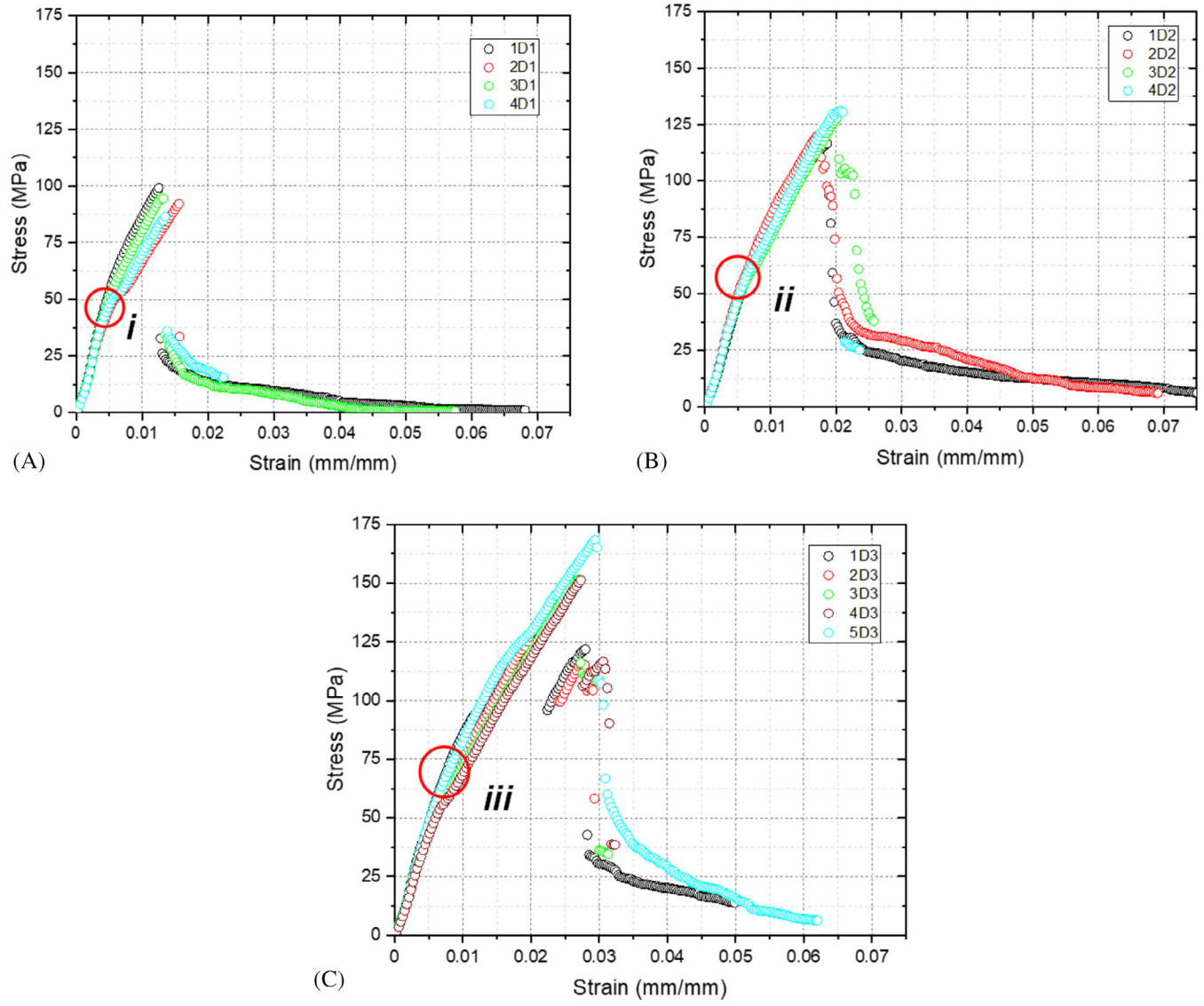

FIGURE 5 Stress–strain curves: (A) laminate XD1–19.5 mm scrap; (B) XD2–39.5 mm scrap; and (C) XD3–59.5 mm.

assembly (how the fiber ends are enclosed) that is related to the quality of the hand layup process as well as the accuracy of the scraps dimensions.

Figure 5A–C, show the curves of laminate type XDY where it is possible to observe a change in the linear region (slopes associated to the axial modulus of elasticity) of each laminate type, related to a bilinear approach. In details *i*, *ii*, and *iii*, it is possible to observe a change in the linear behavior for each fabric length within a well-defined region. The increased fabric length leads to an increase in the stress region where the slopes are reduced, a similar effect to the yielding stress of polymers,[17] which

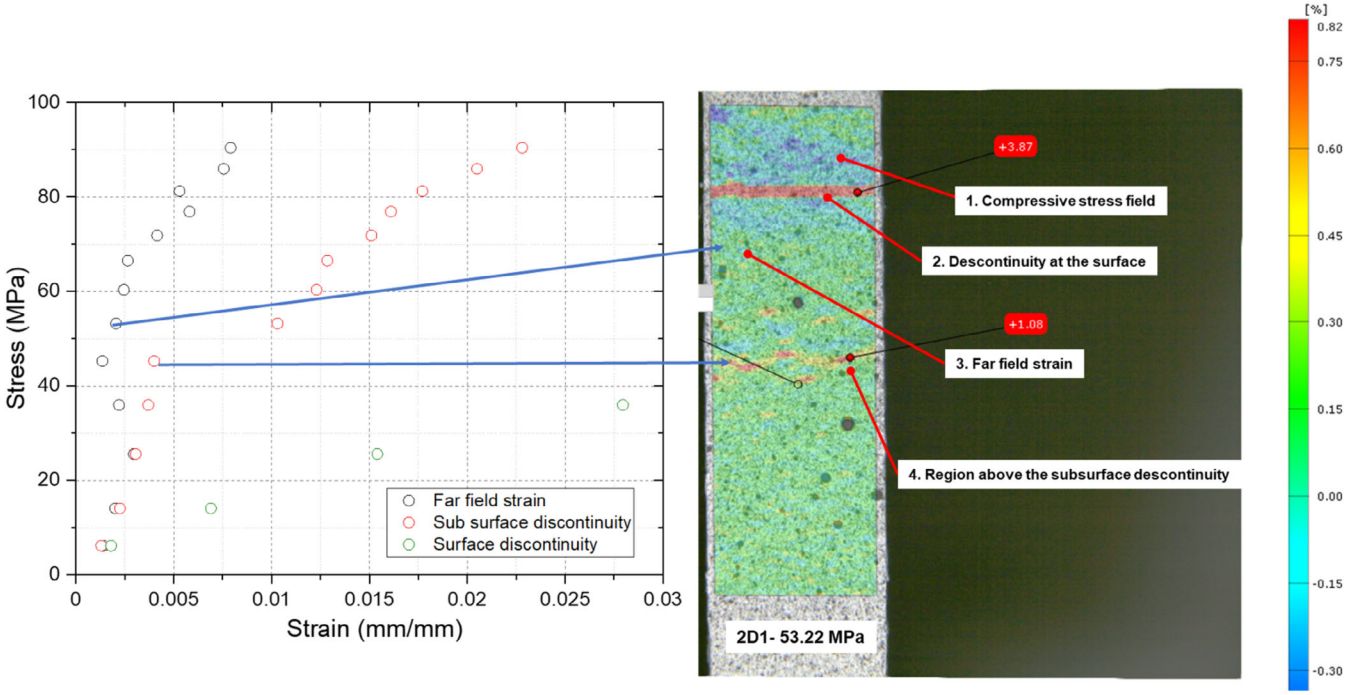

FIGURE 6 Stress–strain curves for laminate type XD1—strain field measurements.

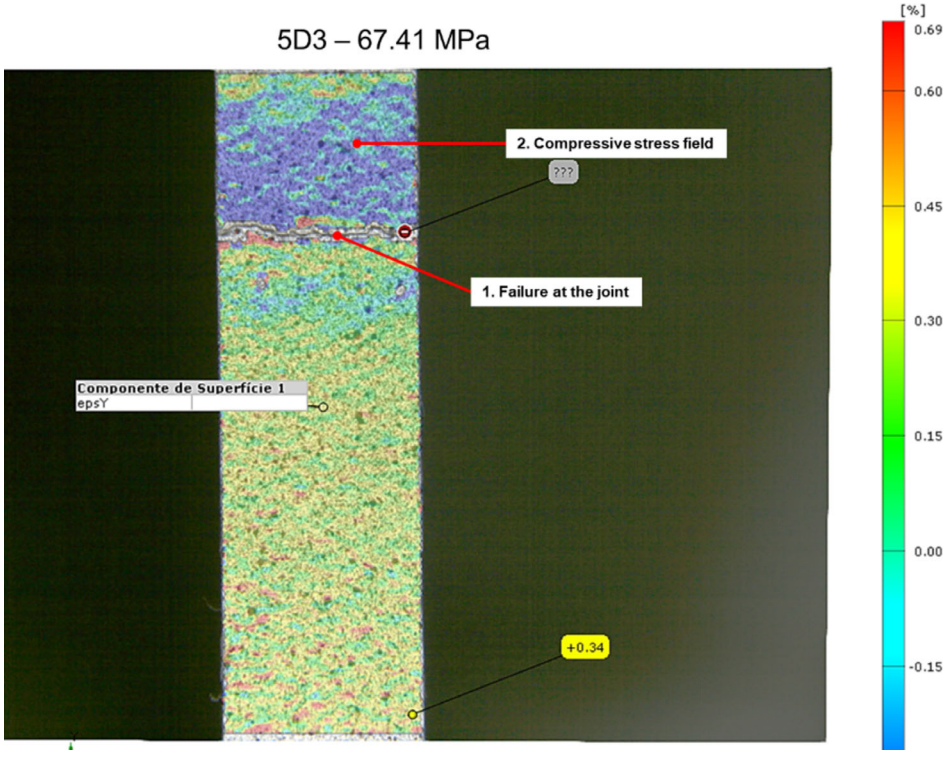

FIGURE 7 Compressive strain field at surface discontinuity.

can be interpreted as an onset slip in between plies (first ply and second ply). In order to explain all the events for both laminates, the strain field over the interrupted section was conducted as depicted in Figure 6.

Figure 6 shows the regions where the values of strain were achieved on the specimen surface. As observed in Figure 5A, the change in the slope was around 50 MPa, and this event is more evident in Figure 6 that starts at 35.93 MPa. The difference between Figures 5A and 6 is that the first represents the average change in the specimen behavior, which is a material that decreases the axial elastic modulus, while the other shown in Figure 6 identifies the local variation of the strain field. The strain field is no longer linearly distributed over the useful area

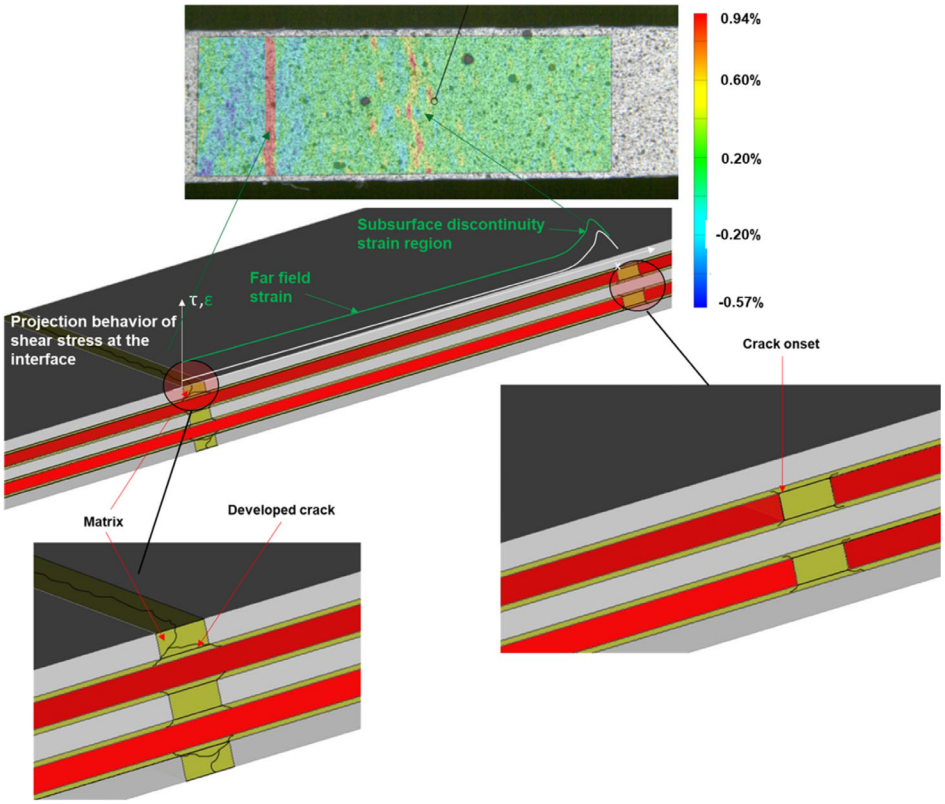

FIGURE 8 Axial stress field with projection of shear stress—graphic adapted from Daniel.[17]

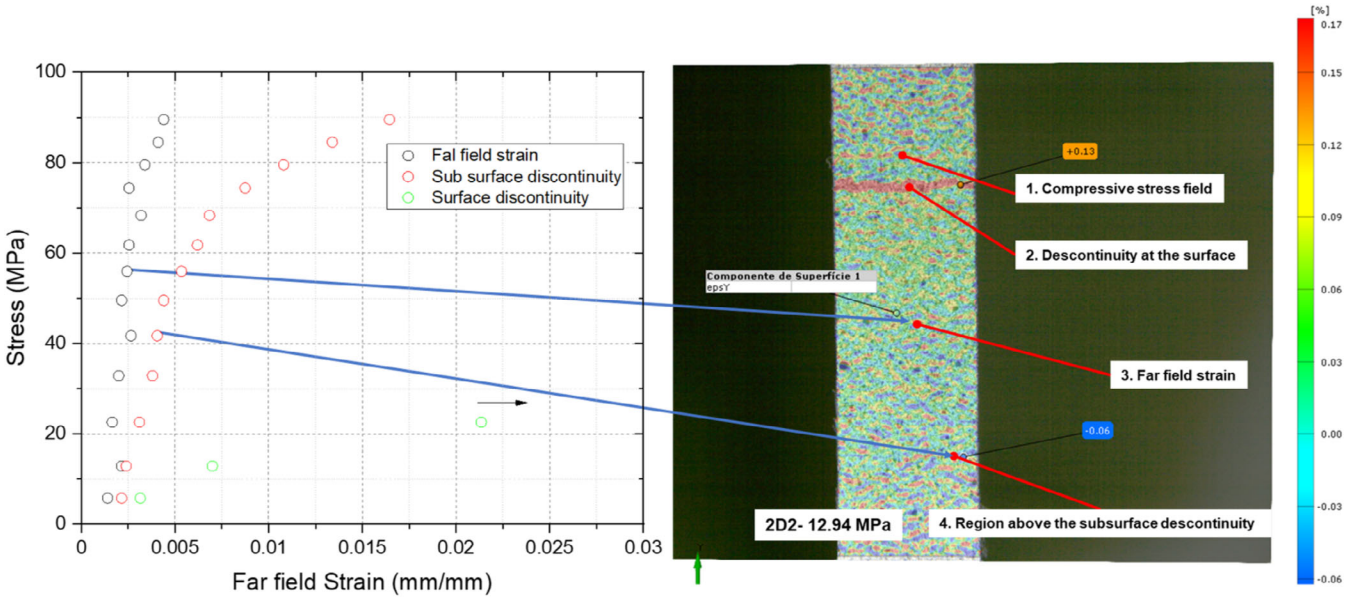

FIGURE 9 Stress–strain curves for laminate type XD2—strain field measurements.

for non-continuous laminate since the strain begins to change according to the presence of the discontinuity (detail 2), creating compression regions (detail 1) due to the different deformation of each layer. Regarding the behavior of the strain field over the subsurface discontinuity (SSD), Figure 6 details 3 and 4, the first point until the third point (25.55 MPa) of the stress–strain curve, the strain was similar in the far field and SSD regions, and at the fourth point, the strain behavior modified.

The strain over the surface discontinuity significantly increases, which can be explained by the polymer strain without the constraint of the reinforcement. Subsequently, the failure occurs (Figure 7—detail 1) and the ply starts to detach, resulting in the peel process. The peeling process provides maximum tensile strength, which is reduced by a combination of stresses, introducing an open delamination mode (present as mixed mode I/II) and also reducing shear strength.[14] Evidence of the peeling process is the presence of compressive strain around the joint, as shown in Figure 7—Detail 2. As the ultimate strength is close to the matrix, the crack initiates and grows between the layers, causing the open delamination due to the asymmetric load distribution.

Previous to failure at the surface discontinuity, the internal discontinuity failure represents the moment the shear forces increase due to the already failed joint at the surface. Then, consequently, the displacement of the two discontinuous layers increased, resulting in a local maximum of strain over the SSD. The increasing difference in strain fields is associated with the already failed surface discontinuity that keeps the far field strain low, with increasing strain at the subsurface discontinuity. These high increments in axial strain at the subsurface discontinuity are due to the local displacement of the joint, which is associated with the shear stress (Figure 8—shear stress versus strain in white color) developed in between layers; this is well established in textbooks for single fiber break.[18,19]

The aforementioned events are schematically represented in Figure 8, which shows the early stages of damages near the joint. Figure 8 also shows the location of the SSD at a stress of 67.05 MPa that as far as from this region, the strain field tends to be even. This region follows the strain from a continuous ply that is bonded to the surface ply; therefore, it constrains the deformation. In advanced stages, the crack at the SSD advances, leading to total delamination, which ceases the loading transferring, resulting in multiple fiber failures.

For the XD2 laminate, the increase in the scrap length (39.5 mm) led to a change in the slope at higher stresses, as observed in Figure 5B, in an overview of the stress–strain curve. An analysis of the strain field

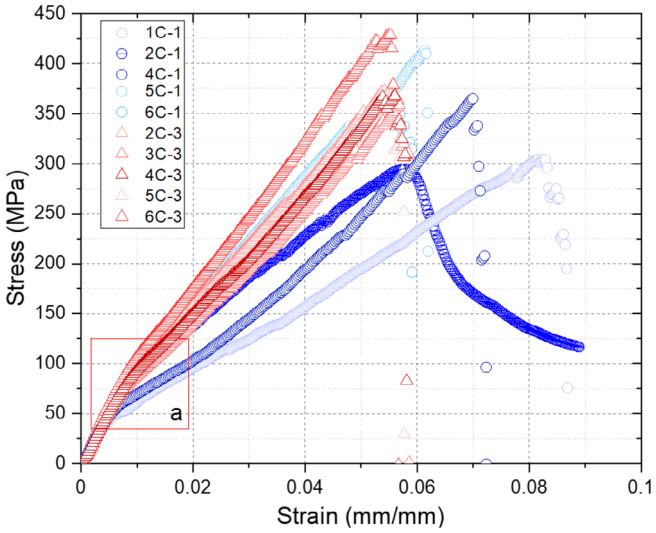

FIGURE 11 Stress–strain curves for the laminate type XCW.

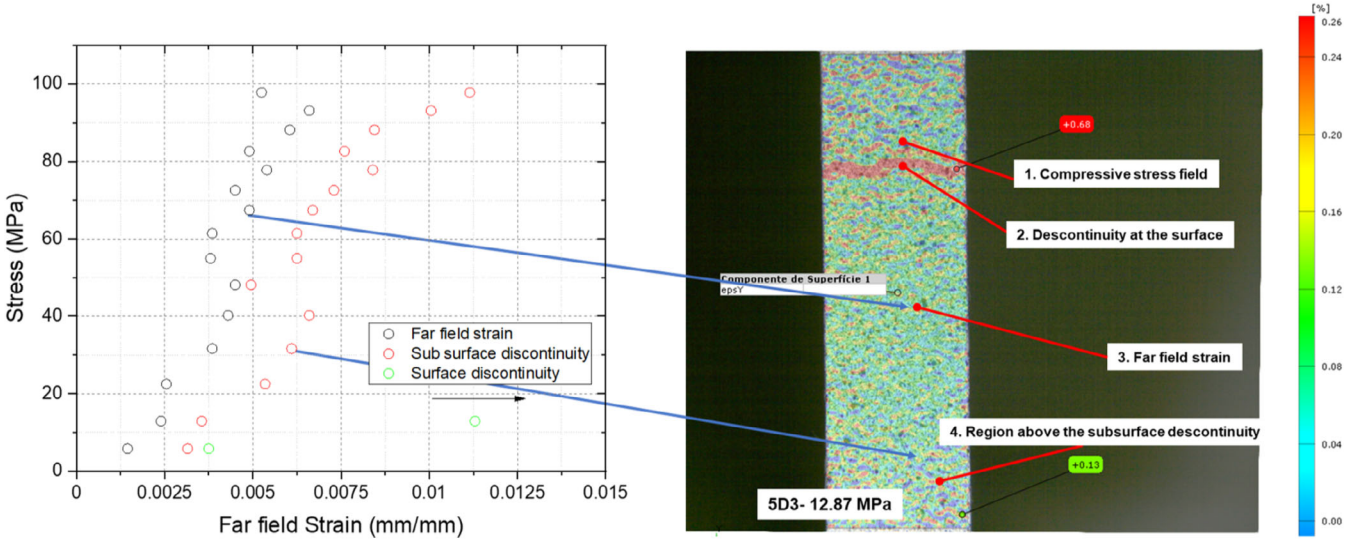

FIGURE 10 Stress–strain curves for laminate type XD3—strain field measurements.

indicates that a difference in strain occurred at 50 MPa, as shown in Figure 9, in a smooth transition as compared to the 19.5 mm scrap length. The difference starts from the second point of the stress–strain curve, suggesting an early difference in strain with smaller maximum axial strain than XD1, thus less intense shear stress. For this particular case, over a region of SSD, the projected a higher critical shear stress than laminate XD1 for delamination propagation. The consequence is that the laminates XD2 hold the stress better, resulting in an increased residual strength (Table 1).

The XD3 laminates showed almost constant strain differences between the two regions which are associated with an integrity of the joint over the SSD region, as seen in Figure 10. The compliance changed at higher stress than the other two laminates at approximately 90 MPa. In this laminate, the SSD was close to the grip region, which might induce some error in the measurement, as the discontinuity is also out of the gage section.

For the laminate type XCW, a higher coefficient of variation was found compared with laminates XDY in the ultimate tensile strength, which can be attributed to an intrinsic variation of carbon fiber strength,[20] as the XCW laminates have 31.2% fiber volume fraction of more continuous fibers than laminate XDY. Laminates XCW presented similar behavior to laminates XDY by increasing fabric length; the tensile strength was improved. This trend is explained by the increase in area for shear force distribution, which requires a higher axial load for interlaminar crack onset and propagation. In Figure 11 detail *a* highlights the change in the slope of the curves, similar to the XDY family. The main difference between the

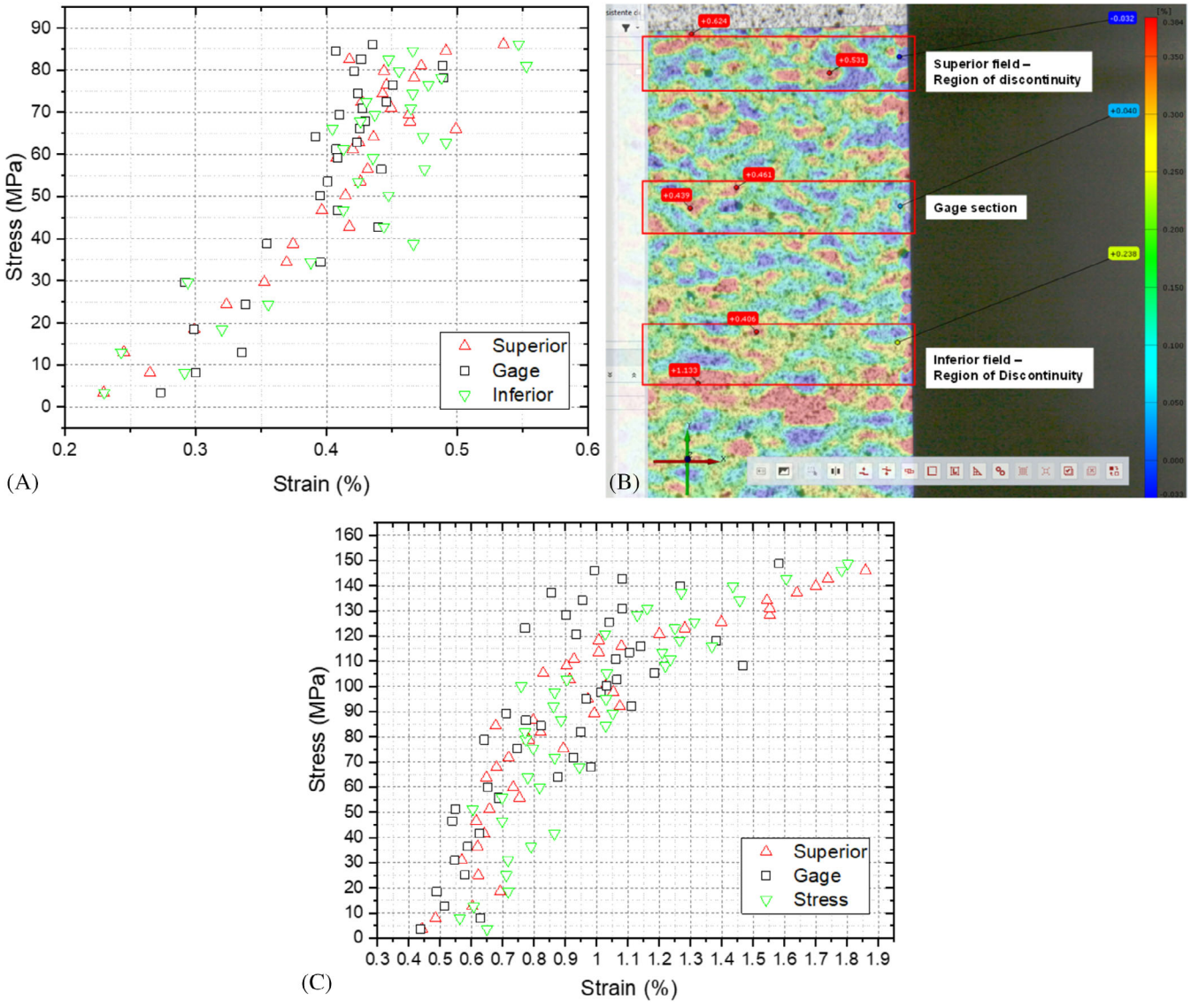

FIGURE 12 Stress–strain curves for laminate type XCW: (A) laminate 4C1; (B) strain field of 4C1; and (C) laminate 5C3.

XDY and XCW is the more evident linear behavior after the transition region, which is attributed to the continuous fabrics.

The analysis of the strain field in Figure 12A,C, enabled us to understand that the strain fields behaved in the same way until the crack onset, which took place when the strain over the SSD was higher than the gage section. The XCW laminate performance was improved by the continuous fibers at the surface, which shield the SSD region, resulting in an even stress transfer around the joint. The crack onset can be noticed at 80 MPa for XC1 laminate (i.e., 19.5 mm), in a region where there is a strain difference, as shown in Figure 12A.

For laminate XC2 (Figure 12C), the change in compliance started at 140 MPa, but all the regions had the same strain. At the moment of joint failure, and in the events that follow, the strain variation remains unaffected by the SSD ply because the layer immediately below it has the same stiffness and therefore provides an equivalent constraint. The continuous laminates adjacent to the cut planes in the central region of the laminate refer to the Central Cut-Ply (CCP), which is essentially designed to obtain the pure shear mode (II), where the stress difference of the internal discontinuous laminates generates slip and the external continuous laminates maintain the pure shear mode.[21] In addition to the stress of the continuous fibers, mode II is the more prone main failure mode for XCW laminates, different from the mixed mode presented in XDY laminates, which is also responsible for the increase in the non-linear and ultimate stress levels.

4 | CONCLUSIONS

This research encompassed the investigation of two types of laminate designed with fiber waste. It was shown that one laminate (XDY) takes advantage of using more fiber waste with different dimensions but is susceptible to failure at the surface, and the subsequent delamination limits the laminate strength. Laminate XCW, with three continuous plies and two discontinuous fibers (waste fibers) presented less severe interlaminar stress conditions that avoid the deterioration of stress transfer between plies. The integrity of the interface in this laminate resulted in improved tensile strength with less influence from the discontinuity position, providing a feasible solution for reusing waste fabric and maintaining mechanical properties. The inspection of the strain field allowed elucidation of the failure events of discontinuous laminate and can contribute to improving layup strategies to prevent stress concentration around the joint.

ACKNOWLEDGMENTS

This study was financed, in part, by the São Paulo Research Foundation (FAPESP), Brazil (Process Numbers #2017/16160-8 and #2023/08798-3).

DATA AVAILABILITY STATEMENT

The data that support the findings of this study are available from the corresponding author upon reasonable request.

REFERENCES

1. Fujii LC, Shiino MY. Development of polyurethane/polyethylene terephthalate/fiber glass polymeric composite from internal auto parts waste. *Prog Rubber Plast Recycl Technol*. 2023;39:64-80.
2. Pakdel E, Kashi S, Varley R, Wang X. Recent progress in recycling carbon fibre reinforced composites and dry carbon fibre wastes. *Resour Conserv Recycl*. 2021;166:105340.
3. Liu P, Meng F, Barlow CY. Wind turbine blade end-of-life options: an eco-audit comparison. *J Clean Prod*. 2019;212:1268-1281.
4. Helbig C, Gemechu ED, Pillain B, et al. Extending the geopolitical supply risk indicator: application of life cycle sustainability assessment to the petrochemical supply chain of polyacrylonitrile-based carbon fibers. *J Clean Prod*. 2016;137:1170-1178.
5. Khalid MY, Arif ZU, Ahmed W, Arshad H. Recent trends in recycling and reusing techniques of different plastic polymers and their composite materials. *Sustainable Mater Technol*. 2022;31:e00382.
6. Singh N, Hui D, Singh R, Ahuja IPS, Feo L, Fraternali F. Recycling of plastic solid waste: a state of art review and future applications. *Compos Part B: Eng*. 2017;115:409-422.
7. Wolfe D. Carbon fiber composite recycling. 2020 https://digitalcommons.cwu.edu/undergradproj/121
8. Carbon Fiber Remanufacturing. Carbon Fiber Remanufacturing (CFR). https://www.carbonfiberremanufacturing.com/pages/company/about.php 2020.
9. Overcash M, Twomey J, Asmatulu E, Vozzola E, Griffing E. Thermoset composite recycling—driving forces, development, and evolution of new opportunities. *J Compos Mater*. 2018;52:1033-1043.
10. Chen J, Wang J, Ni A. Recycling and reuse of composite materials for wind turbine blades: an overview. *J Reinf Plast Compos*. 2019;38:567-577.
11. Kelly A, Tyson WR. Tensile properties of fibre-reinforced metals: copper/tungsten and copper/molybdenum. *J Mech Phys Solids*. 1965;13:329-350.
12. Pegoretti A. Recycling concepts for short-fiber-reinforced and particle-filled thermoplastic composites: a review. *Adv Ind Eng Polym Res*. 2021;4:93-104.
13. Van Hattum FWJ, Bernardo CA. A model to predict the strength of short fiber composites. *Polym Compos*. 1999;20:524-533.
14. Shiino MY, Monticeli FM, Donadon MV. Limited strength of short fiber composites: identification of variables affecting the critical fiber length. *J Compos Mater*. 2023;57:1927-1940.
15. Vas LM, Ronkay F, Czigány T. Active fiber length distribution and its application to determine the critical fiber length. *Polym Test*. 2009;28:752-759.
16. ASTM International. ASTM D3039/D3039M. *Annual Book of ASTM Standards*. ASTM International; 2014:1-13. doi:10.1520/D3039
17. Raghava R, Caddell RM, Yeh GSY. The macroscopic yield behaviour of polymers. *J Mater Sci*. 1973;8:225-232.

18. Daniel IM, Ishai O. *Engineering Mechanics of Composite Materials*. Oxford University Press; 2006.
19. Jones R. *Mechanics of Composite Materials*. McGraw-Hill; 1975.
20. Yu W, Yao J. Tensile strength and its variation of PAN-based carbon fibers. I. Statistical distribution and volume dependence. *J Appl Polym Sci*. 2006;101:3175-3182.
21. Baldassarre A, Martinez M, Rans C. Residual stress evaluation of adhesively bonded composite using central cut plies specimens. *J Adhes*. 2020;96:1355-1384.

How to cite this article: Shiino MY, Albernaz GG, dos Santos YB, Monticeli FM. Discontinuous laminate composites manufactured with fiber waste: Design approaches and failure analysis. *Polym Compos*. 2025;1-11. doi:10.1002/pc.29828